Hindawi Publishing Corporation
International Journal of Distributed Sensor Networks
Volume 2012, Article ID 893739, 11 pages
doi:10.1155/2012/893739

Research Article

Field Measurement of Wind Characteristics of Typhoon Muifa on the Shanghai World Financial Center

Y. An, Y. Quan, and M. Gu

State Key Laboratory of Disaster Reduction in Civil Engineering, Tongji University, Shanghai 200092, China

Correspondence should be addressed to M. Gu, minggu@tongji.edu.cn

Received 29 June 2012; Accepted 26 August 2012

Academic Editor: Hong-Nan Li

Field measurement is considered to be the most reliable method to obtain wind characteristics of typhoon, and it is of essential value of further understanding of wind-resistant design of super tall buildings. In this paper, the wind data were recorded atop the Shanghai World Financial Center (SWFC) with a height of 494 m during the whole course of Typhoon Muifa on August 6–8 in 2011. Detailed analysis of the field data is conducted to investigate the characteristics of the typhoon-generated wind including the mean wind speed and direction, turbulence intensities, gust factors, peak factors, turbulence integral length scales, and spectra of fluctuating wind speed. A comparative study between the measured wind characteristics and those previously obtained in the literature is also carried out. It is found that the average values of turbulence intensities, gust factors, and turbulence integral length scales under the condition of Typhoon Muifa are higher than those under monsoon condition atop the SWFC, and Von Karman spectra are suitable to describe of the turbulent kinetic energy distribution at Lujiazui of the Pudong district in Shanghai.

1. Introduction

As a destructive disastrous weather system, typhoon has been threatening China for thousands of years, especially in southern China. Typhoons that have landed in China account for about 35% of the total number that developed in Northwest Pacific area. Based on the statistical results on available typhoon records since 1949 by Shanghai Meteorological Administration, it is indicated that the intensity of tropical cyclones landing in China follows an upward trend, where the proportion of strong typhoon increases every year as well. Thus, it is of essential value to investigate wind characteristics for further understanding of wind-resistant design of tall buildings [1].

Although many advances in wind tunnel tests and numerical simulation techniques have been recognized, there are still many critical phenomena which can only be investigated by full-scale experiments. Field measurement is considered to be the most reliable method of evaluating wind characteristics of tall buildings, and it will be the fundamental approach for a long term. Some countries have developed local database of wind characteristics, such as Frøya database in Norway [2], offshore observation databases in Canada and the United Kingdom, Sparks database in the USA, and the extensive results observed by Kato et al. [3] in Japan. In Hong Kong and mainland China, several measurement results of wind effects have been contributed by Li et al. [4–6], Xu and Zhan [7], Gu et al. [8, 9], and Li et al. [10, 11]. However, field study of wind effects on super tall buildings under typhoon conditions is still far from sufficient.

At present, the lack of field data is an obstructive factor in the development of research of the wind characteristics. Some field measurements of typhoon effects on skyscrapers have been carried out in Southern China, but few were conducted in Shanghai due to the fact that typhoons rarely move to such high latitude. Thus, field measurements of typhoon-generated wind data in Shanghai are of great value for the understanding of wind characteristics in eastern China.

The wind data were recorded atop the 494 m high Shanghai World Financial Center during the whole course of Typhoon Muifa on August 6–8 in 2011. Detailed analysis of the field data was conducted to investigate the characteristics of the typhoon-generated wind including the turbulence

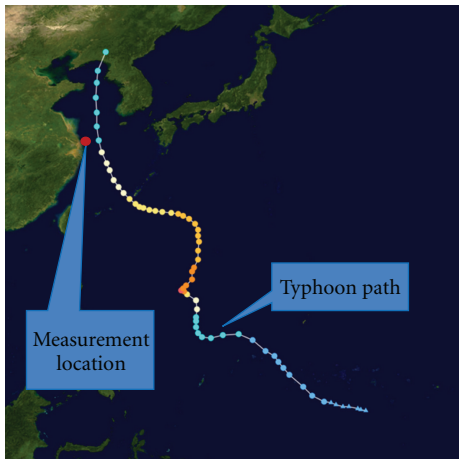

Figure 1: Storm path of Typhoon Muifa (from Wikipedia).

Figure 2: Overview of the SWFC.

intensities, gust factors, peak factors, turbulence integral length scales, and spectra of fluctuating wind speed.

2. Typhoon Muifa

Typhoon Muifa was a large, strong, and persistent typhoon. It was the ninth named storm of the 2011 Pacific typhoon season. Early on July 28, the tropical storm, named Muifa, entered the Philippine. The storm gradually drifted north over the next day while maintaining tropical storm strength. At 08:00 on July 30, Muifa was upgraded into a Severe Tropical Storm; the storm strengthened rapidly and was upgraded into a typhoon at 14:00 and a strong typhoon at 20:00. Muifa had strengthened to a super typhoon in the next day when the sustained wind speed reached 55 m/s and weakened to strong typhoon later in the day. The storm gradually moved north and was finally downgraded into a severe tropical storm on August 7. After weakening to a tropical storm, Muifa made landfall at North Korea on August 8. Early on August 9, Muifa weakened to a tropical depression in northeast China and became a low-pressure area later. During the passage of Typhoon Muifa, the minimum horizontal distance between the observation site and the typhoon center was 260 km. Figure 1 shows the storm path of Typhoon Muifa.

3. Overview of the Measurement

The Shanghai World Financial Center (SWFC), located in the Pudong district of Shanghai, is the tallest skyscraper in mainland China, whose structure height is 492 m, as shown in Figure 2. The building is surrounded by a large number of tall and super tall buildings, making the wind characteristics of atmospheric surface layer of the building extremely complex.

According to a preliminary CFD simulation of the wind field around the SWFC, the wind data are interfered by the parapet walls and the window clean machines assembled atop the SWFC. To obtain as many available data as possible, two spots for wind speed observation were located at two corners atop the building, namely, northeast side and southwest side, as shown in Figure 3. Two ultrasonic anemometers (Figure 4) were installed at each spot at a height of 494 m from the ground level. The horizontal distance between the ultrasonic anemometers is 71.6 m. In this study, x-axis, y-axis, and z-axis are defined as the north, west, and upward directions of the ultrasonic anemometer respectively, as illustrated in Figure 5. By this way, the wind direction increases with anticlockwise direction from the top view. For instance, the wind direction from the south is 0 degree, and from the east is 90 degrees. The measurement range of the ultrasonic anemometer is from 0.01 to 65 m/s, with the maximum dynamic response frequency of 40 HZ and the actual sampling frequency of 10 HZ. The real-time storage of the acquired data is achieved by CR1000 data acquisition system program produced by Campbell Scientific, Inc. Among the acquired data, those within a wind direction range of 45 degrees at each side atop the SWFC are considered as the available data, based on the CFD simulation.

4. Approach to Analysis of Wind Data

4.1. Mean Wind and Direction. The wind speed of x-axis, y-axis, and z-axis, denoted by $u_x(t)$, $u_y(t)$, and $u_z(t)$, respectively, can be measured by ultrasonic anemometers simultaneously. Since $u_x(t)$, $u_y(t)$, and $u_z(t)$ are time series of x-axis, y-axis, and z-axis, the longitudinal, lateral, and vertical components of wind speed can be obtained by means of vector decomposition method.

Making 10 min the averaging time interval, the mean horizontal wind speed U and the mean horizontal wind direction φ are

$$U = \sqrt{\overline{u_x(t)}^2 + \overline{u_y(t)}^2},$$
$$\cos(\phi) = \frac{\overline{u_x(t)}}{U}. \quad (1)$$

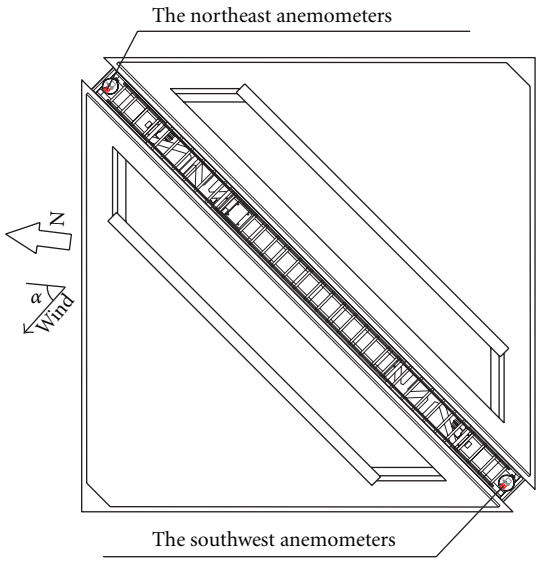

Figure 3: Sketch of the location of the ultrasonic anemometers.

Figure 4: WindMaster Pro ultrasonic anemometers.

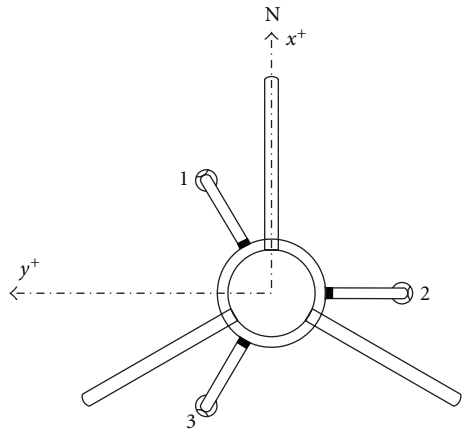

Figure 5: Definition of x, y, and z axes of the anemometer.

The direction of vertical wind speed is the same as that of z-axis; thus, the mean vertical wind speed W is

$$W = \overline{u_z(t)}. \tag{2}$$

The longitudinal, lateral, and vertical components of fluctuating wind speed within a basic time interval, denoted by $u_x(t)$, $u_y(t)$ and $u_z(t)$, can be obtained as follows:

$$\begin{aligned} u(t) &= u_x(t)\cos\phi + u_y(t)\sin\phi - U, \\ v(t) &= -u_x(t)\sin\phi + u_y(t)\cos\phi, \\ w(t) &= u_z(t) - W. \end{aligned} \tag{3}$$

4.2. Turbulence Intensity, Gust Factor, and Peak Factor. The turbulence intensity (I) indicates the variation of wind speed as well as the relative intensity of the fluctuating wind. It is defined as the ratio of standard deviation of fluctuating wind speed within 10 min to the mean horizontal wind speed U, expressed as

$$I_i = \frac{\sigma_i}{U} \quad (i = u, v, w), \tag{4}$$

where $\sigma_i\,(i = u, v, w)$ is the standard deviation of fluctuating wind speeds $u(t)$, $v(t)$, and $w(t)$ within the analyzed time interval, respectively.

The gust factors demonstrate proportions of gust wind speed to mean wind speed. It is generally defined as the ratio of maximum mean wind speed during gust duration t_g, which is usually made as 3 s in structural wind engineering, to mean horizontal wind speed U in 10 min. G_u can be obtained by

$$G_u\left(t_g\right) = 1 + \frac{\max\left(\overline{u\left(t_g\right)}\right)}{U}, \qquad G_v\left(t_g\right) = \frac{\max\left(\overline{v(t_g)}\right)}{U},$$
$$G_w\left(t_g\right) = \frac{\max\left(\overline{w\left(t_g\right)}\right)}{U}, \tag{5}$$

where $\max(\overline{u(t_g)})$, $\max(\overline{v(t_g)})$, and $\max(\overline{w(t_g)})$ are the maximum mean wind speeds of longitudinal, lateral, and vertical directions during gust duration t_g, respectively.

Similar to the gust factor, the peak factor also features the instantaneous intensity of the fluctuating wind, which can be calculated from

$$g_u = \frac{\hat{U}_{t_g} - U}{\sigma_u}, \tag{6}$$

where $\hat{U}_{t_g}$ is the maximum mean wind speed within time interval t_g, and σ_u is the standard deviation of $u(t)$.

4.3. Turbulence Integral Length Scale. The turbulence integral length scale (L^x) is one of the important parameters for describing the turbulent characteristics of wind flows, and it is generally interpreted as the length of the dominating

vortex scale. It varies from different analysis methods. Of the methods developed by numerous researchers, two effective approaches are usually adopted to calculate the turbulence scale: the first one is autocorrelation function integral method based on Taylor hypothesis [12], expressed by (7); the other one is Von Karman velocity spectrum method used to fit the measured velocity spectrum as the fitting parameter, expressed in (8). The fluctuating wind speed in the former method is assumed to be stable, while in the latter the velocity spectrum must fit Von Karman velocity spectrum. In this paper, the turbulence scale is calculated using the former method

$$L_i^x = \frac{U}{\sigma_i^2} \int_0^\infty R_i(\tau) d\tau \quad (i = u, v, w), \tag{7}$$

$$L_i^x = \frac{US_i(0)}{4\sigma_i^2} \quad (i = u, v, w). \tag{8}$$

In (7) and (8), $R_i(\tau)\,(i = u, v, w)$ is the autocorrelation function of fluctuating wind; $S_i(0)\,(i = u, v, w)$ is the fluctuating wind spectrum value when $f = 0$; $\sigma_i^2\,(i = u, v, w)$ is the variance of fluctuating wind speed.

4.4. Power Spectral Density of Fluctuating Wind Speed. The power spectral density of fluctuating wind speed describes the contribution of the kinetic energy of the vortices in different sizes to the whole turbulent kinetic energy. The values of spectrum in the frequency domain represent the distributive ratios of the kinetic energy of different vortices to the turbulent kinetic energy. Davenport Spectrum, Von Karman Spectrum, Simiu Spectrum, Kaimal Spectrum, and Harris Spectrum are some typical fitting power spectra, among which the Von Karman form has been widely recognized as a suitable representation of velocity spectra [13]. Equation (9) is the expressions of normalized Von Karman spectra [14]:

$$\begin{aligned} \frac{nS_\varepsilon(n)}{{\sigma_\varepsilon}^2} &= \frac{4nL_\varepsilon^x/U}{\left[1 + 70.8\left(nL_\varepsilon^x/U\right)^2\right]^{5/6}} \quad (\varepsilon = u), \\ \frac{nS_\varepsilon(n)}{\sigma_\varepsilon^2} &= \frac{4nL_\varepsilon^x/U\left[1 + 755.2\left(nL_\varepsilon^x/U\right)^2\right]}{\left[1 + 283\left(nL_\varepsilon^x/U\right)^2\right]^{11/6}} \quad (\varepsilon = v, w), \end{aligned} \tag{9}$$

where n is the frequency; $L_\varepsilon\,(\varepsilon = u, v, w)$ is the turbulence integral length scales in the longitudinal, lateral, and vertical directions, respectively; $S_\varepsilon(n)\ (\varepsilon = u, v, w)$ is the power spectral density of the fluctuating wind components in the longitudinal, lateral, and vertical direction, respectively.

5. Characteristics of Typhoon Muifa

5.1. Mean Wind Speed and Direction. Based on the preanalysis of the whole time histories of wind speed measured at both sides atop the SWFC when Typhoon Muifa passed Shanghai, a 42-hour time history measured at the northeast side, from 0:00 on August 6 to 18:00 on August 7, is chosen as research sample. Figure 6 shows the variations of mean wind speed and mean wind direction in each 10-min period at both sides atop the SWFC during the passage of Muifa. According to the Chinese Load Code for the Design of Building Structures [15], the research object is divided into 252 consecutive samples with an averaging time interval of 10 minutes. The maximum 10-min mean wind speed reaches 32.97 m/s, which illustrates that the strength of Muifa is intense, and can also be attributed to that the building site is 260 km far from the center of the typhoon. Figure 7 shows the signal time histories of the research sample along three axes of ultrasonic anemometer. In addition, with respect to the samples, variations of the mean wind speed and mean wind direction in each 10 min period as well as the time histories of longitudinal, lateral, and vertical fluctuating components are shown in Figures 8 and 9.

5.2. Turbulence Intensity. As an important parameter to describe the characteristics of fluctuating wind speed and determine design wind loads on structures, it is of significant value to investigate the turbulence intensity under typhoon condition. Before calculating turbulence intensities, unwanted data among those 252 samples caused by unfavorable effect of parapet walls and window clean machines on the anemometers are filtered out by means of the effective wind angle which is determined by CFD simulation of the flow field. Variations of the longitudinal, lateral, and vertical turbulence intensities I_u, I_v, and I_w with 10 min mean wind speed are illustrated in Figure 10. The minimum, maximum, and average values are 0.05, 0.29, and 0.14 for I_u; 0.04, 0.26, and 0.13 for I_v; 0.04, 0.17, and 0.09 for I_w, respectively. It is observed that all the turbulence intensity components I_u, I_v, and I_w remain almost constant with 10 min mean wind speed, among which, I_u exhibits the most scattered character.

Comparison results of the ratios between the three average values of the turbulence intensities in the longitudinal, lateral, and vertical direction in this study with available field measurement results in the literature are listed in Table 1. Li et al. [4, 11] conducted field measurement atop the Jin Mao Building with a height of 420.5 m during the passage of Typhoon Rananim, and the average values of the longitudinal and lateral turbulence intensities with a time interval of 10 min were 0.562 and 0.437, respectively, while those measured in Hong Kong during the passage of Typhoon Sally were 0.216 and 0.206, respectively [5], all of which are higher than the results in this study. Xu and Zhan [7] found that the mean longitudinal turbulence intensity in 1 hr period atop the Di Wang Tower during the passage of Typhoon York was 0.117, which was slightly lower than the lateral one. Gu et al. [9] analyzed the wind data recorded atop the SWFC under monsoon condition, and the average values of longitudinal and lateral turbulence intensities were 0.085 and 0.075, which, compared with results in this study, shows that the turbulence intensities under typhoon condition are higher than those under monsoon condition at Lujiazui of the Pudong district in

Table 1: Comparison of the ratios between the three average values of the turbulence intensities in the longitudinal, lateral, and vertical directions.

Reference	Type of wind field	Observation height (m)	$I_u : I_v : I_w$ ($I_u : I_v$)	Location
Solari and Piccardo [14]	/	/	1 : 0.75 : 0.55	/
Tieleman [16]	Monsoon	5	1 : 0.80 : 0.39	The Netherlands
Shiau and Chen [17]	Typhoon Babs	26	1 : 0.78 : 0.50	Taiwan (China)
Li et al. [5]	Typhoon Sally	325	1 : 0.95	Shenzhen (China)
		374	1 : 0.27	Hong Kong (China)
Li et al. [4]	Typhoon Rananim	420	1 : 0.78	Shanghai (China)
Gu et al. [9]	Monsoon	494	1 : 0.88	Shanghai (China)
Cao et al. [1]	Typhoon Maemi	10	1 : 0.83 : 0.56	Japan
Pang and Ling [18]	Typhoon Jelawat	20	1 : 0.54 : 0.23	Shanghai (China)
	Typhoon Prapiroon		1 : 0.91 : 0.46	
Wang et al. [19]	Typhoon Muifa	10	1 : 0.67 : 0.50	Shanghai (China)
		20	1 : 0.65 : 0.55	
		40	1 : 0.73 : 0.47	
This paper	Typhoon Muifa	494	1 : 0.93 : 0.64	Shanghai (China)

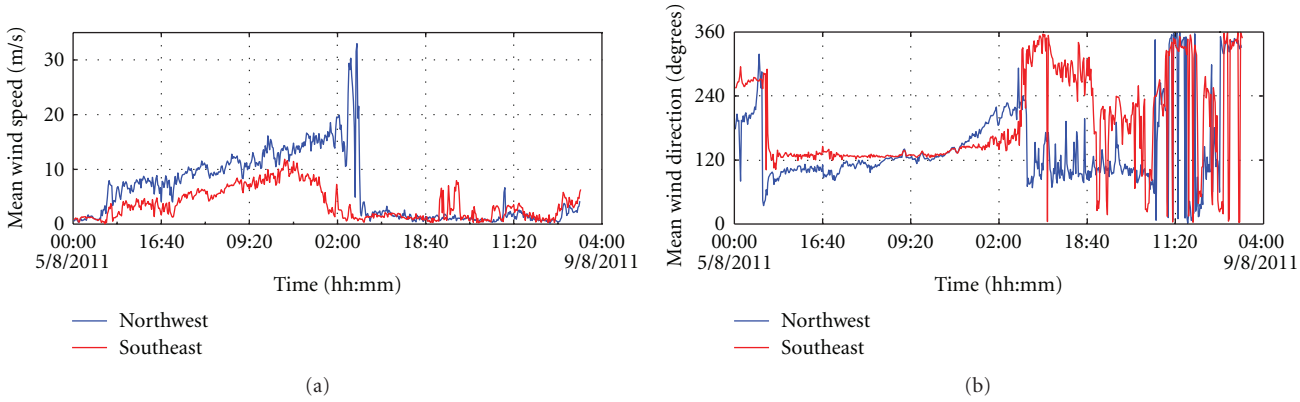

Figure 6: Variation of 10 min mean wind speeds and mean wind directions (top) Shanghai World Financial Center.

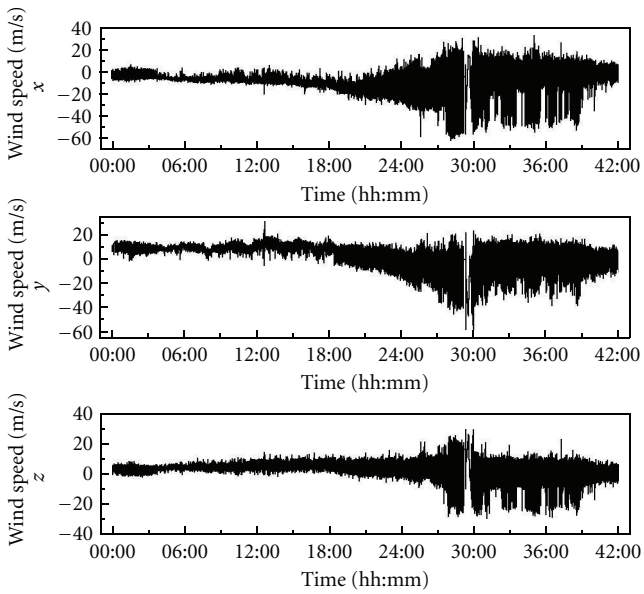

Figure 7: Ultrasonic anemometer signal histories along three axes of the samples.

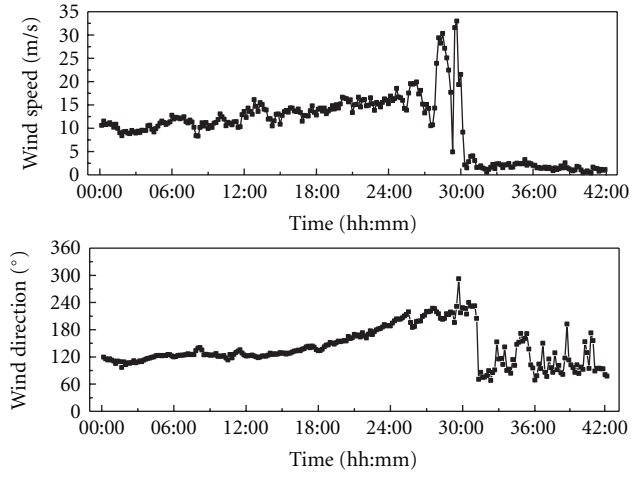

Figure 8: Variation of mean wind speed and mean wind direction.

Shanghai. This can be attributed to the differences of characteristics between typhoon and monsoon. Furthermore, of the same height, 0.115 is recommended by the Architectural Institute of Japan (AIJ) Recommendation for Loads on

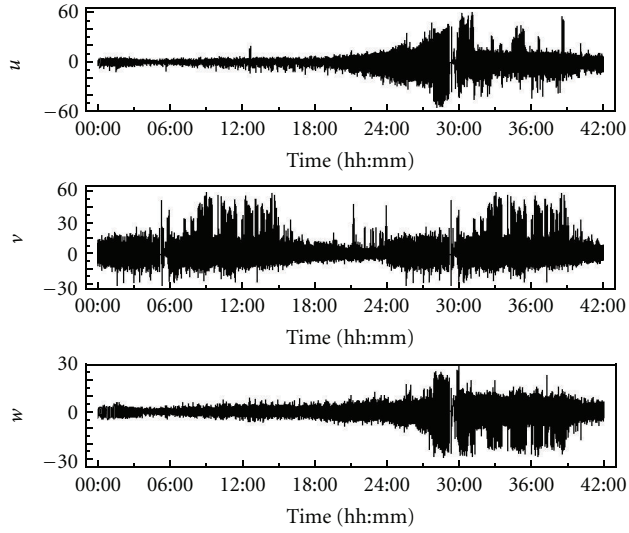

Figure 9: Time histories fluctuating wind in the longitudinal, lateral, and vertical directions.

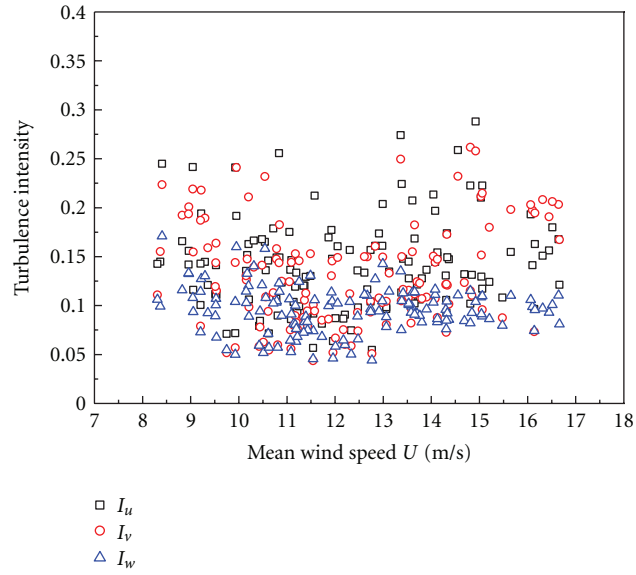

Figure 10: Variation of turbulence intensities with 10 min mean wind speed in three directions.

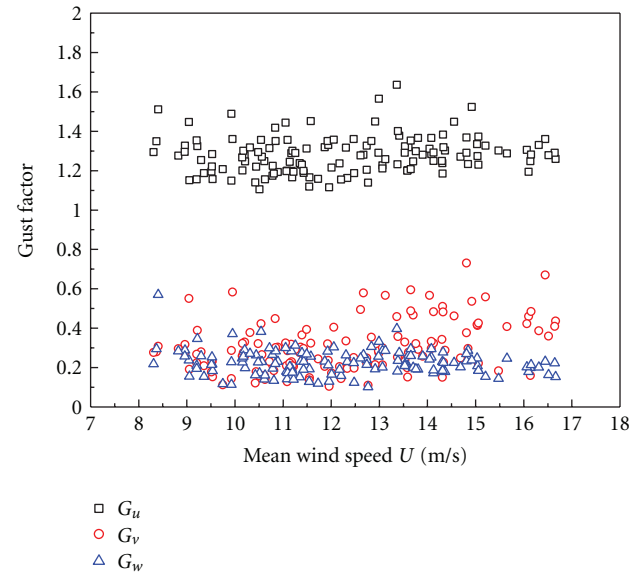

Figure 11: Variation of gust factors with 10 min mean wind speed in three directions.

Buildings [21] for longitudinal turbulence intensity under the similar type of site. Comparing the recommended value with the observed one in this paper, it is found that the former is slightly smaller than the latter, suggesting that the longitudinal turbulence intensity recommended by the Recommendation for Loads on Buildings [21] is no longer applicable under typhoon condition at a height of 494 m. Although there is no explicit equations for turbulence intensities in the Chinese Load Code for the Design of Building Structures [15], yet with respect to a fluctuating coefficient in the code and the definition of turbulence intensity, an equivalent value of 0.036 can be calculated, which is much lower than the measured value in this study and the recommended value in the AIJ-2004. Thus, the Chinese code is obviously conservative for turbulence intensities.

5.3. Gust Factor. Similar to turbulence intensity, the gust factor is also an important parameter to describe the characteristics of fluctuating wind and to determine wind-induced dynamic response of structures [4, 11]. By analyzing the effective samples, the longitudinal, lateral, and vertical gust factors with a gust duration of 3 s in 10 min period are obtained. Figure 11 presents the variation of longitudinal, lateral, and vertical gust factors G_u, G_v, and G_w with 10 min mean wind speed. The minimum, maximum, and average values are 1.11, 1.64, and 1.28 for G_u; 0.10, 0.73, and 0.31 for G_v; and 0.10, 0.57, and 0.22 for G_w, respectively. It is shown that the gust factors in the three directions, G_u, G_v, and G_w remain almost constant with mean wind speed. Gu et al. [9] found that the average values of longitudinal and lateral gust factors were 1.15 and 0.17 atop the SWFC under monsoon condition, which were slightly lower than those in this study, and there is a tendency for the gust factors to decrease with the increase of mean wind speed. This can be attributed to the same reason as discussed previously for the turbulence intensity. During the passage of Typhoon Muifa, a field study carried out by Wang et al. [19] at elevation of 10 m on an observation tower located in the Pudong district shows that the average values of longitudinal, lateral, and vertical gust factors are 1.48, 0.30, and 0.29 at 10 m, respectively, among which the longitudinal, and vertical gust factors are higher than those in the present study.

5.4. Peak Factor. The peak factor with a gust duration of 3 s in 10 min period is analyzed. Figure 12 shows the variation of the peak factor with 10 min mean wind speed. It can be seen that all the points lie approximately on a horizontal line,

Table 2: Comparison of the ratios between the three average values of the turbulence integral length scale in the longitudinal, lateral, and vertical directions.

Reference	Type of wind field	Observation height (m)	$L_u : L_v : L_w$
Kato et al. [3]	Typhoon	55.7	1 : 0.33 : 0.17
		86.0	1 : 0.50 : 0.17
Gu et al. [8]	Monsoon	494	1 : 0.90 : 0.42
Hui et al. [20]	Monsoon	50	SW 1 : 0.36 : 0.098
Wang et al. [19]			NE 1 : 0.46 : 0.19
	Typhoon	10	1 : 0.54 : 0.07
		20	1 : 0.65 : 0.11
		40	1 : 0.73 : 0.1
This paper	Typhoon	494	1 : 0.54 : 0.42

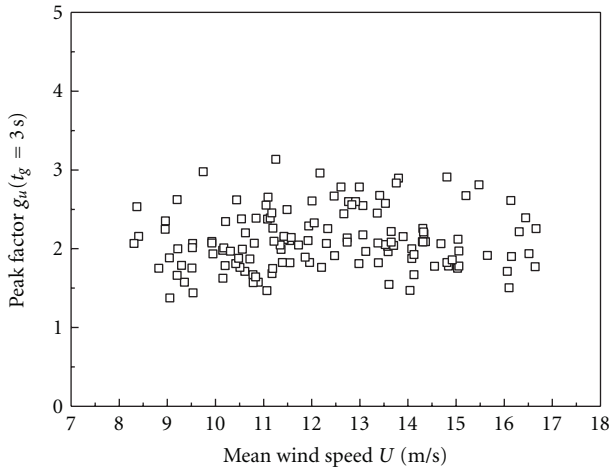

Figure 12: Variation of peak factor with 10 min mean wind speed.

and the minimum, maximum, and average values of peak factors are 1.37, 3.13, and 2.11, respectively. The average peak factors derived from the field study by Wang et al. [19] at elevation of 10 m, 20 m, and 40 m on an observation tower in Pudong district during the passage of Typhoon Muifa are 3.18, 3.16, and 3.05, respectively, which are slightly higher than the results in the present study.

5.5. Turbulence Integral Length Scale. Values for the longitudinal, lateral, and vertical turbulence integral length scales of the effective samples are obtained from integration of the autocorrelation function. Figures 13(a), 13(b), and 13(c) show the variation of the longitudinal, lateral, and vertical turbulence integral length scales with the 10 min mean wind speed. It is observed that the turbulence integral length scales in the longitudinal direction scatter with the increase of 10 min mean wind speed and no explicit trend can be found between them. While the turbulence integral length scales in the other two directions remain almost constant with the increase of 10 min mean wind speed. The minimum, maximum, and average values are 37.24 m, 706.77 m, and 217.60 m for L_u; 39.16 m, 459.14 m, and 117.98 m for L_v; and 18.74 m, 488.24 m, and 54.17 m for L_w, respectively. In addition, it is noticed that the average values of L_u, L_v and L_w measured atop the SWFC under monsoon condition were 127.98 m, 114.85 m, and 54.17 m [8], respectively; those obtained by Wang et al. [19] at elevation of 40 m on an observation tower in Pudong district during the passage of Typhoon Muifa were 150.31 m, 110.24 m, and 14.94 m respectively. All of them in the corresponding directions are lower than the measured values in the present study. On the other hand, as specified in the Recommendation for Loads on Buildings [21], the longitudinal turbulence integral length scale can be estimated by the following empirical equation:

$$L_u = \begin{cases} 100\left(\dfrac{Z}{30}\right)^{0.5}, & 30 < Z \le Z_G, \\ 100, & Z \le 30\,\text{m}, \end{cases} \tag{10}$$

where Z is the observation height; Z_G is the height of the gradient wind. And the recommended value atop the SWFC determined by (10) is 405.79 m, which is much higher than the average observed value in the present study (217.60 m), suggesting that (7) employed in the Recommendation for Loads on Buildings [21] does not suit the estimation of the longitudinal turbulence integral length scale atop the SWFC during the passage of Typhoon Muifa.

Comparison results of the ratios between the three average values of the turbulence intensities in the longitudinal, lateral, and vertical directions in this study with available field measurement results in the literature are listed in Table 2. It is noteworthy that the ratio of $L_u : L_v$ in this study is consistent with the one from Wang et al. [19] at elevation of 10 m during the passage of Typhoon Muifa. Meanwhile, the ratio of $L_u : L_w$ in this study is obviously higher than those from Wang et al. [19]. The main reason for this discrepancy can be attributed to that the present field measurements of wind data atop the SWFC were conducted at a height of 494 m above ground level and the results provided in Wang et al. [19] were obtained near ground. Moreover, the ratio of $L_u : L_w$ in this study is in good agreement with the one from Gu et al. [8] atop the SWFC under monsoon condition, while the ratio of $L_u : L_v$ in this study is noticeably lower than the one from Gu et al. [8], which may be attributed to the differences between the turbulence structures of

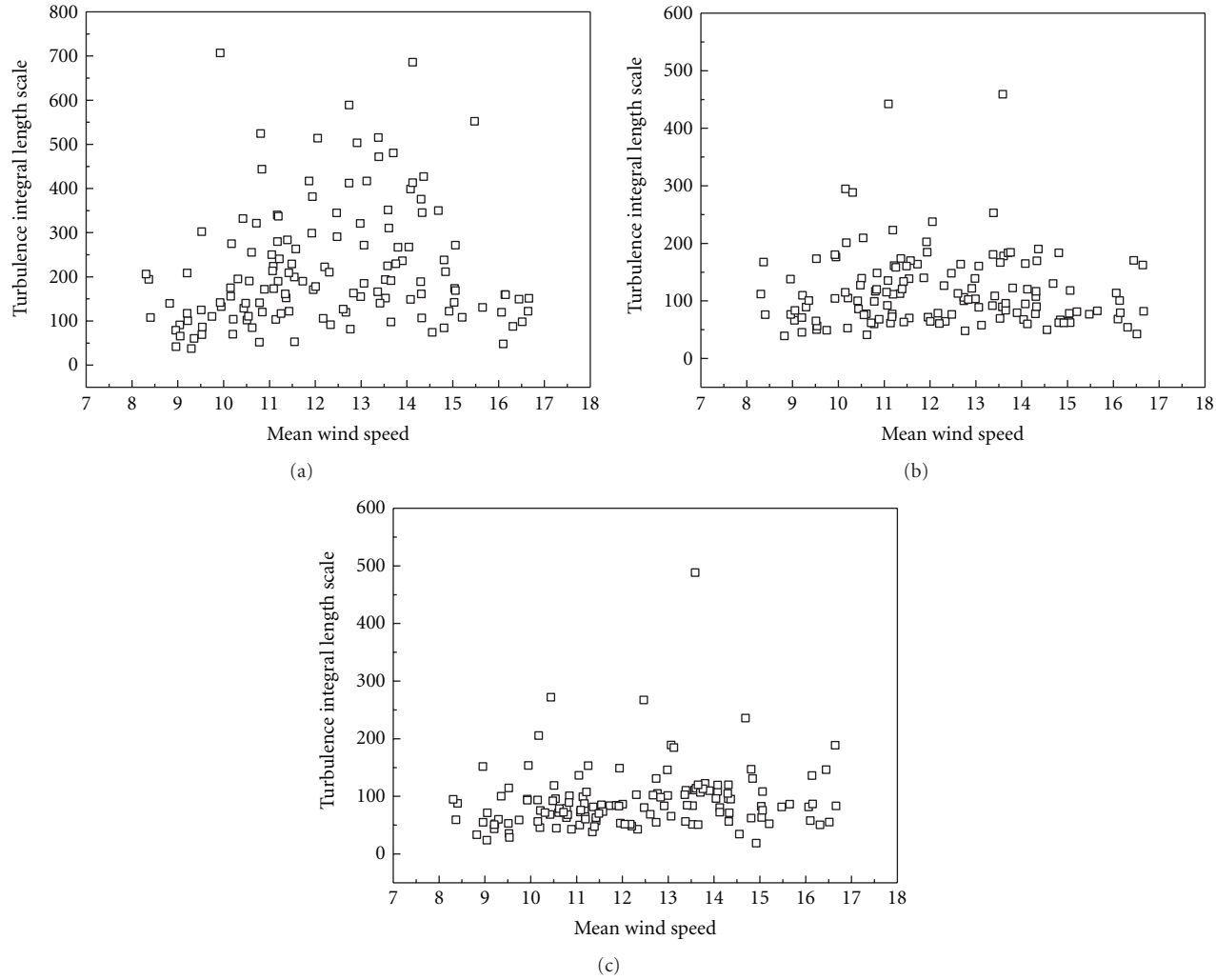

Figure 13: Variation of turbulence integral length scales with 10 min mean wind speed in three directions: (a) longitudinal turbulence integral length scale, (b) lateral turbulence integral length scale, and (c) vertical turbulence integral length scale.

typhoon and monsoon. In view of this, the factors that may influence turbulence integral length scales lie in the type of atmospheric flow, height of observation, terrain conditions and wind speed, and so forth.

5.6. Power Spectral Density of Fluctuating Wind Speed. The power spectral density can significantly affect the wind-induced dynamic responses of tall buildings and it is, thus, worthwhile to identify the power spectral density functions based on the field measured wind speeds [5]. The normalized autopower spectral density functions of the fluctuating wind speed in the longitudinal, lateral, and vertical directions are obtained from the wind data measured atop the SWFC during the passage of Typhoon Muifa, as shown in Figures 14(a), 14(b), and 14(c). It is observed that the shapes of the spectra obtained from three different samples disagree to some extent. Within low-frequency range, the spectra of the different samples fit fairly well, while within inertial subrange, the value of the spectrum increases with the increasing 10 min mean wind speed. Thus, it is indicated that turbulent kinetic energy distributes mainly in the low-frequency region, and the dissipation rate of turbulent kinetic energy decreases with the increasing 10 min mean wind speed within inertial subrange.

The measured spectra in the longitudinal, lateral, and vertical directions and the corresponding Von Karman spectra using the measured-turbulence integral length scales are presented in Figures 15(a), 15(b), and 15(c) for comparison purposes. It can be observed that the measured spectral density functions of fluctuating wind speed in the longitudinal, lateral, and vertical directions fit fairly well with the Von Karman spectra using the measured turbulence integral length scales, indicating that the Von Karman spectra are suitable for the description of the turbulent kinetic energy distribution at Lujiazui of the Pudong district in Shanghai.

6. Conclusions

The wind data were recorded atop the 494 m high Shanghai World Financial Center during the whole course of Typhoon Muifa on August 6–8 in 2011. Detailed analysis of the

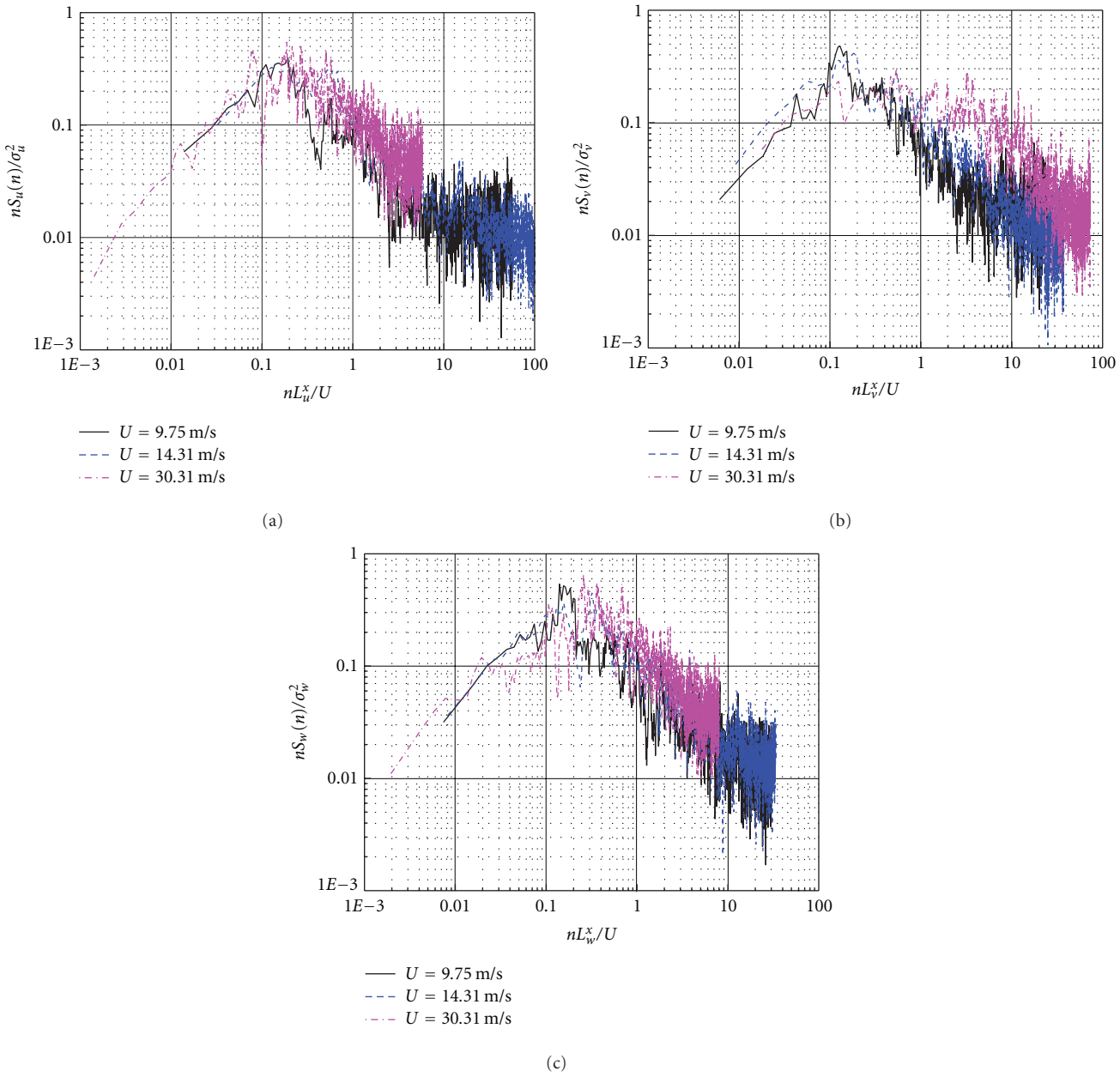

FIGURE 14: The normalized autopower spectral density functions of the fluctuating wind speed: (a) longitudinal spectra, (b) lateral spectra, and (c) vertical spectra.

field data was conducted to investigate the characteristics of the typhoon-generated wind including the turbulence intensities, gust factors, peak factors, turbulence integral length scales, and spectra of fluctuating wind speed. Some important conclusions are listed as follows.

(1) All the turbulence intensity components I_u, I_v, and I_w remain almost constant with 10 min mean wind speed, among which, I_u exhibits the most scattered character. The average values of I_u, I_v and I_w are 0.14, 0.13, and 0.09, respectively, which are higher than those obtained by Gu et al. [9] at the same site under monsoon condition. The longitudinal turbulence intensities recommended by the Recommendation for Loads on Buildings [21] and the Chinese Load Code for the Design of Building Structures [15] are no longer applicable for engineering purpose.

(2) The gust factors in the three directions, G_u, G_v, and G_w remain almost constant with mean wind speed, and the average values of G_u, G_v, and G_w are 1.28, 0.31, and 0.22, respectively, which are higher than those obtained by Gu et al. [9] at the same site under monsoon condition. The average values of longitudinal and vertical gust factors obtained by Wang et al. [19] at elevation of 10 m on an

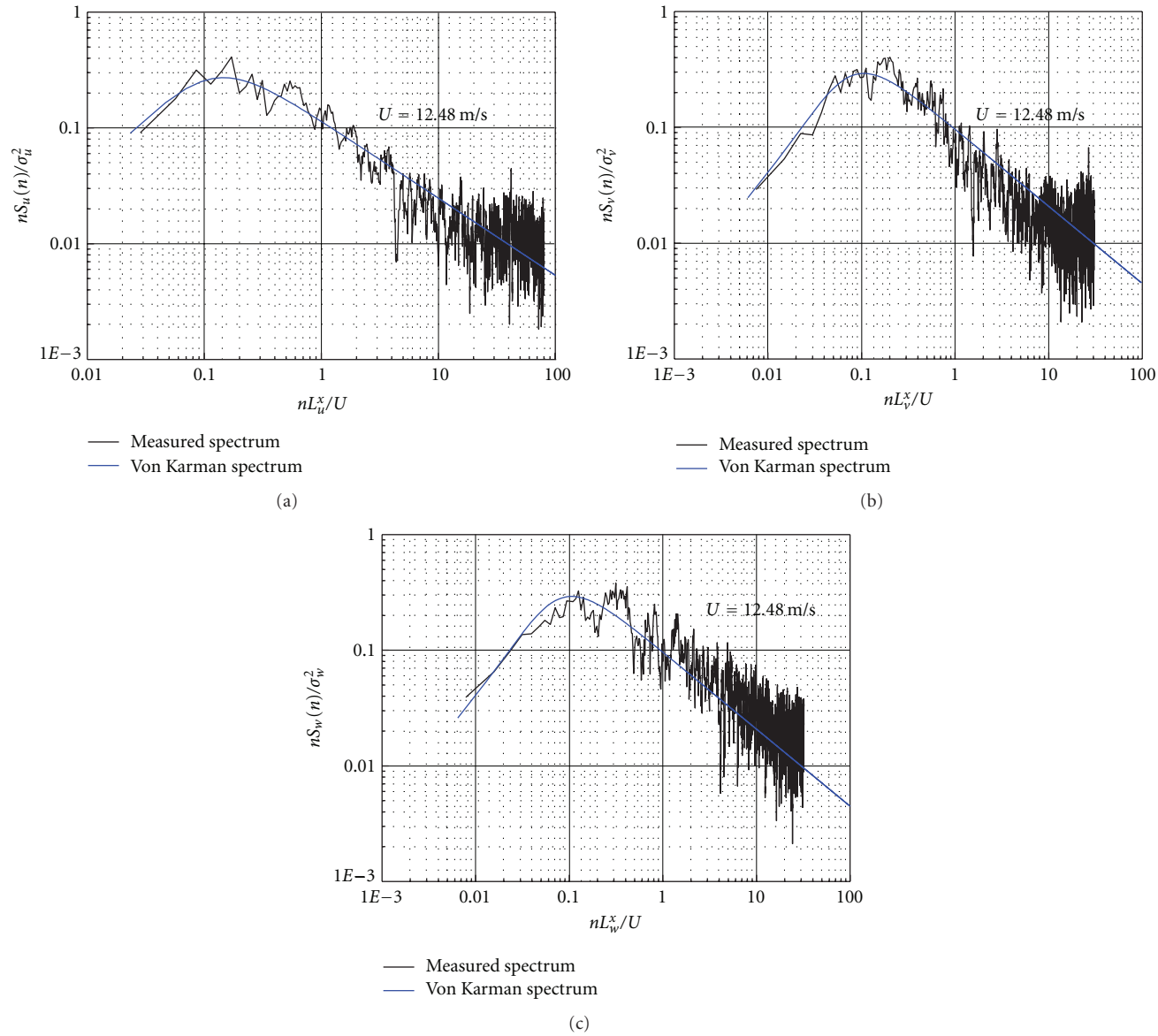

Figure 15: Comparison between the measured spectra and Von Karman spectra: (a) longitudinal spectrum, (b) lateral spectrum, and (c) vertical spectrum.

observation tower located in the Pudong district during the passage of Typhoon Muifa are higher than those in this study.

(3) All the peak factors lie approximately on a horizontal line with the increasing 10 min mean wind speed, and the minimum, maximum, and averages value of peak factors are 1.37, 3.13, and 2.11, respectively. The average gust factors obtained by Wang et al. [19] at elevation of 10 m, 20 m, and 40 m are slightly higher than those in this study.

(4) The turbulence integral length scales in the longitudinal direction scatter with the increase of 10 min mean wind speed and those in the other two directions remain almost constant with the increase of 10 min mean wind speed. The average values of L_u, L_v, and L_w are 217.60 m, 117.98 m, and 54.17 m, respectively, all of which are higher than those obtained by Gu et al. [8] and Wang et al. [19]. Equation (7) employed in the Recommendation for Loads on Buildings [21] does not suit the estimation of the longitudinal turbulence integral length scale atop the SWFC during the passage of Typhoon Muifa.

(5) The shapes of the spectra obtained from three different samples disagree to some extent. Within low-frequency range, the spectra of the different samples fit fairly well, while within inertial subrange, the values of the spectra increase with the increasing 10 min mean wind speed. The turbulent kinetic energy distributes mainly in the low-frequency region, and the dissipation rate of turbulent kinetic

energy decreases with the increasing 10 min mean wind speed within inertial subrange. The measured spectra fit fairly well with the Von Karman spectra using the measured turbulence integral length scales, indicating that the Von Karman spectra are suitable for the description of the turbulent kinetic energy distribution at Lujiazui of the Pudong district in Shanghai.

Acknowledgment

The work presented in this study is supported by the National Natural Science Foundation (90715040), which is gratefully acknowledged.

References

[1] S. Cao, Y. Tamura, N. Kikuchi, M. Saito, I. Nakayama, and Y. Matsuzaki, "Wind characteristics of a strong typhoon," *Journal of Wind Engineering and Industrial Aerodynamics*, vol. 97, no. 1, pp. 11–21, 2009.

[2] O. J. Andersen and J. Løvseth, "The Frøya database and maritime boundary layer wind description," *Marine Structures*, vol. 19, no. 2-3, pp. 173–192, 2006.

[3] N. Kato, T. Ohkuma, J. R. Kim, H. Marukawa, and Y. Niihori, "Full scale measurements of wind velocity in two urban areas using an ultrasonic anemometer," *Journal of Wind Engineering and Industrial Aerodynamics*, vol. 41, no. 1–3, pp. 67–78, 1992.

[4] Q. S. Li, Y. Q. Xiao, J. Y. Fu, and Z. N. Li, "Full-scale measurements of wind effects on the Jin Mao building," *Journal of Wind Engineering and Industrial Aerodynamics*, vol. 95, no. 6, pp. 445–466, 2007.

[5] Q. S. Li, Y. Q. Xiao, and C. K. Wong, "Full-scale monitoring of typhoon effects on super tall buildings," *Journal of Fluids and Structures*, vol. 20, no. 5, pp. 697–717, 2005.

[6] Q. S. Li, Y. Q. Xiao, J. R. Wu, J. Y. Fu, and Z. N. Li, "Typhoon effects on super-tall buildings," *Journal of Sound and Vibration*, vol. 313, no. 3–5, pp. 581–602, 2008.

[7] Y. L. Xu and S. Zhan, "Field measurements of Di Wang tower during typhoon York," *Journal of Wind Engineering and Industrial Aerodynamics*, vol. 89, no. 1, pp. 73–93, 2001.

[8] M. Gu, J. Kuang, Y. Quan, X. Wei, and L. J. Xiong, "Analysis of measured wind speed data on top of SWFC," *Journal of Vibration and Shock*, vol. 28, no. 12, pp. 114–118, 2009 (Chinese).

[9] M. Gu, J. Kuang, X. Wei, L. Xiong, and Y. Quan, "Field measurement of strong wind speed of normal climate on top of Shanghai World Financial Center," *Journal of Tongji University (Natural Science)*, vol. 39, no. 11, pp. 1592–1597, 2012 (Chinese).

[10] H. Li, T. Yi, Q. Jing, L. Huo, and G. Wang, "Wind-induced vibration control of dalian international trade mansion by tuned liquid dampers," *Mathematical Problems in Engineering*, vol. 2012, Article ID 848031, 21 pages, 2012.

[11] H. N. Li, T. H. Yi, X. D. Yi, and G. X. Wang, "Measurement and analysis of wind-induced response of tall building based on GPS technology," *Advances in Structural Engineering*, vol. 10, no. 1, pp. 83–93, 2007.

[12] R. G. J. Flay and D. C. Stevenson, "Integral length scales in strong winds below 20 m," *Journal of Wind Engineering and Industrial Aerodynamics*, vol. 28, no. 1–3, pp. 21–30, 1988.

[13] Y. Tamura, A. Kareem, G. Solari, K. C. S. Kwok, J. D. Holmes, and W. H. Melbourne, "Aspects of the dynamic wind-induced response of structures and codification," *Wind and Structures*, vol. 8, no. 4, pp. 251–268, 2005.

[14] G. Solari and G. Piccardo, "Probabilistic 3-D turbulence modeling for gust buffeting of structures," *Probabilistic Engineering Mechanics*, vol. 16, no. 1, pp. 73–86, 2001.

[15] "GB50009-2001, Load code for the design of building structures," Beijing, China, 2002.

[16] H. W. Tieleman, "Strong wind observations in the atmospheric surface layer," *Journal of Wind Engineering and Industrial Aerodynamics*, vol. 96, no. 1, pp. 41–77, 2008.

[17] B. S. Shiau and Y. B. Chen, "In situ measurement of strong wind velocity spectra and wind characteristics at Keelung coastal area of Taiwan," *Atmospheric Research*, vol. 57, no. 3, pp. 171–185, 2001.

[18] J. Pang and Z. Ling, "Field measurements of strong wind characteristics near ground in Pudong district," *Experiments and Measurements in Fluid Mechanics*, vol. 16, no. 3, pp. 32–39, 2002 (Chinese).

[19] X. Wang, P. Huang, and M. Gu, "Field measurements about integral scales of near-ground turbulence during Typhoon 'Muifa"' (Chinese), *Journal of Tongji University*. In press.

[20] M. C. H. Hui, A. Larsen, and H. F. Xiang, "Wind turbulence characteristics study at the Stonecutters Bridge site: part II: wind power spectra, integral length scales and coherences," *Journal of Wind Engineering and Industrial Aerodynamics*, vol. 97, no. 1, pp. 48–59, 2009.

[21] "Architectural institute of Japan, Recommendations for loads on buildings," Japan, 2004.